Available online at www.sciencedirect.com
ScienceDirect
Nuclear Instruments and Methods in Physics Research B 266 (2008) 1154–1161
NIM B
Beam Interactions with Materials & Atoms
www.elsevier.com/locate/nimb

Semi-empirical dielectric descriptions of the Bethe surface of the valence bands of condensed water

D. Emfietzoglou [a], I. Abril [b], R. Garcia-Molina [c], I.D. Petsalakis [d], H. Nikjoo [e], I. Kyriakou [a], A. Pathak [f,*]

[a] Medical Physics Laboratory, University of Ioannina Medical School, Ioannina 451 10, Greece
[b] Department de Física Aplicada, Universitat d'Alacant, Apartat 99, E-03080 Alacant, Spain
[c] Departmento de Física - CIOyN, Universidad de Murcia, Apartado 4021, E-30080 Murcia, Spain
[d] Theoretical and Physical Chemistry Institute, The National Hellenic Research Foundation, Athens 116 35, Greece
[e] Center for Advanced Space Studies, USRA, NASA Johnson Space Center, Houston TX 77058, USA
[f] School of Physics, University of Hyderabad, Hyderabad 500 046, India

Received 18 September 2007; received in revised form 27 November 2007
Available online 5 December 2007

Abstract

The Bethe surface of a material is an essential element in the study of inelastic scattering at low impact energies where the optical approximation fails. In this work we examine various semi-empirical models for the dielectric response function of condensed water towards an improved description of the energy-loss function over the whole energy–momentum plane (i.e. Bethe surface). The experimental "optical" data (i.e. at zero momentum transfer) for the valence bands of liquid and solid water are analytically represented by a sum-rule constrained linear combination of Drude-type functions. The dependence on momentum transfer is introduced through various widespread "extension" schemes which are compared against the available Compton scattering data. It is shown that the widely used Lindhard function along with its "single-pole" (or "δ-oscillator") approximation used in the Penn and Ashley models, as well as the Ritchie and Howie extended-Drude scheme with a simple quadratic dispersion, predict a sharp Bethe ridge which compares poorly with the experimental profile. In contrast, the Mermin dielectric function provides a more realistic account of the observed broadening with momentum transfer. An improved *fully*-extended-Drude model is presented which incorporates the momentum broadening and line-shift of the Bethe ridge and distinguishes between the different dispersion of the discrete and continuum spectra of water.

PACS: 71.10.Ca; 71.15.Dx; 71.15.Mb

Keywords: Inelastic scattering; Bethe surface; Bethe ridge; Dielectric function; Energy loss function; Water; Ice

1. Introduction

The study of inelastic scattering of swift charges by atoms/molecules in both the gas and condensed phase, is largely pursued within the plane-wave Born approximation (PWBA) which provides a consistent theoretical framework over a substantial part of the electronic regime [1]. Moreover, if supplemented with appropriate correction terms, the PWBA may provide fairly accurate inelastic and stopping cross sections down to the Bragg peak region [2]. The only non-trivial parameter in this methodology is a material-dependent term which reflects the response of the target to the external perturbation and defines the so-called *Bethe surface* [3]. Depending on whether the target atoms/molecules are in the gas or condensed phase, it is customary to define the Bethe surface as a three-dimensional plot over the energy–momentum plane of either the atomic/molecular generalised-oscillator-strength (GOS) or the solid-state energy-loss function (ELF), respectively [3]. Formally, both the GOS and ELF depend on the initial

* Corresponding author. Tel.: +91 40 23010181/23134316; fax: +91 40 23010181/23010227.
E-mail address: appsp@uohyd.ernet.in (A. Pathak).

0168-583X/$ - see front matter © 2007 Elsevier B.V. All rights reserved.
doi:10.1016/j.nimb.2007.11.057

and final state many-electron wavefunctions. Thus, apart from the free-electron-gas and the atomic hydrogen where close analytic forms exist, the calculation of the ELF (or GOS) from first-principles is, up to this date, a formidable task for practical applications [2].

The above state of affairs has motivated work on semi-empirical models which try to circumvent the perplexities of a theoretical many-body calculation by taking advantage the direct connection of the ELF (or GOS) to measurable properties of the material. Perhaps the most popular approach is to use experimental "optical" data (i.e. at zero momentum transfer) to describe the dependence on energy transfer and simple dispersion (extension) schemes to incorporate the dependence on momentum transfer [4]. These so-called extended-optical-data models are expected to provide a computationally simple, yet accurate, representation of the ELF over the whole Bethe surface. Ritchie and Howie [5] advanced the extended-Drude scheme whereby the momentum dependence is implemented directly into the Drude coefficients, whereas Penn [6], Ashley [7] and Fernandez-Varea et al. [8] have employed various approximations to the Lindhard dielectric function [9]. More recently, in an effort to improve upon the Lindhard-based models, Garcia-Molina, Abril and co-workers [10] have applied the Mermin dielectric function [11] which provides a theoretically more consistent account of the dependence on momentum transfer.

With respect to condensed water, Emfietzoglou and co-workers [12–16] have provided a comprehensive review and intercomparison of various extended-optical-data models and advanced an improved scheme for both the liquid and solid phase [14,16]. The new development is based on an effective parameterization of the available inelastic X-ray scattering (IXS) data [17,18] by means of a *fully*-extended-Drude (FED) model in the Ritchie and Howie sense. Contrary to all earlier experimental data for condensed water which are restricted to the optical limit, the IXS (Compton) data extend to finite values of momentum transfer providing, for the first time, an empirical test for dispersion models.

In the present work we study various aspects of the Bethe surface of condensed water based on the application of the Drude, Lindhard and Mermin dielectric functions. In particular, we concentrate on the momentum dependence of the dielectric function which dictates the Bethe ridge profile. We restrict our study to the valence bands where condensed phase effects are expected to be dominant and the dielectric theory most justified. The present work is relevant to inelastic calculations at low impact energies (e.g. Bragg peak region) where the optical-approximation fails and should be substituted by various integrals over the Bethe surface.

2. Methodology

2.1. The extended-Drude dielectric function

The extended-Drude model has been particularly popular mainly because of its applicability to a broad range of materials and the convenient analytic properties of the Drude function. Following Ritchie and Howie [5] the experimental optical-ELF is analytically represented by a sum of Drude-type functions:

$$\mathrm{Im}\left[\frac{-1}{\varepsilon(E,q=0)}\right]_{\mathrm{exp}}=\sum_j A_j D(E,\Gamma_j,\Omega_j), \tag{1}$$

where ε is the dielectric response function, E and q are the transferred energy and momentum, respectively, A_j, Γ_j and Ω_j are coefficients associated with the strength, damping and transition energy, respectively, of each electronic channel j and "D" denotes the Drude function:

$$D(E,\Gamma_j,\Omega_j)=\frac{\Gamma_j E}{\left(\Omega_j^2-E^2\right)^2+\left(\Gamma_j E\right)^2}. \tag{2}$$

Ritchie and Howie [5] suggested an empirical determination of the above coefficients based on the amplitude (A_j), width (Γ_j) and position (Ω_j) of each peak in the deconvolution of the experimental spectrum. The extension to the momentum space may then be obtained by appropriate dispersion relations for all or some of the coefficients, e.g. using $\Gamma_j(q)=\Gamma(\Gamma_j,q)$ and $\Omega_j(q)=\Omega(\Omega_j,q)$ where q is the momentum transfer. In general, the particular analytic expression for the momentum dependence should be found empirically. The most popular form of the Ritchie and Howie [5] model overcomes the requirement of any parametric fitting beyond the optical limit by adopting a pure quadratic dispersion relation for the energy-coefficient while keeping the rest of the coefficients independent of q:

$$\mathrm{Im}\left[\frac{-1}{\varepsilon(E,q)}\right]=\sum_j A_j D(E,\Gamma_j,\Omega_j(q)), \tag{3a}$$

$$\Omega_j(q)=\Omega_j+\frac{q^2}{2m_{\mathrm{e}}}, \tag{3b}$$

where m_{e} is the electron mass. Besides its simplicity, Eq. (3b) is correct at the two limiting cases of $q\to 0$ and $q\to\infty$ where $\Omega_j(q)$ approaches its optical value, $\Omega_j(q=0)$ and the free-electron kinematic value corresponding to the Bethe ridge, $q^2/2m_{\mathrm{e}}$, respectively. Also, for materials where the Fermi and plasmon energies do not differ appreciably, Eq. (3b) resembles the plasmon dispersion of the free-electron gas at small-q. Recent applications of the above version of the Ritchie and Howie model may be found in Leger et al. [19], Akkerman et al. [20] and Tung et al. [21].

For condensed water, the availability of experimental data for all dielectric function representations, namely, $\mathrm{Re}(\varepsilon)=\varepsilon_1$, $\mathrm{Im}(\varepsilon)=\varepsilon_2$ and $\mathrm{Im}(-1/\varepsilon)$, has motivated the development of somewhat more elaborate representations of its dielectric response properties where basic band structure characteristics are accounted for [12–16,22]. In the study of liquid [12–15] and solid [16] water the following set of equations has been adopted to represent the experimental data. For the imaginary part of the dielectric function we use:

$$\mathrm{Im}[\varepsilon(E,q=0)]_{\mathrm{exp}}=\sum_j \varepsilon_2^{(D)}(E,q=0;f_j,E_j,\gamma_j)=\begin{cases}\sum\limits_j^{\mathrm{ioniz}} D_2(E,f_j,E_j,\gamma_j)+\sum\limits_j^{\mathrm{excit}}\tilde{D}_2(E,f_j,E_j,\gamma_j), & \text{for} \quad E>B_{\mathrm{ioniz,min}}\\ \sum\limits_j^{\mathrm{excit}}\tilde{D}_2(E,f_j,E_j,\gamma_j), & \text{for} \quad B_{\mathrm{excit,min}}\leqslant E<B_{\mathrm{ioniz,min}}\end{cases}, \tag{4}$$

where

$$D_2(E,f_j,E_j,\gamma_j)=E_{\mathrm{p}}^2\frac{f_j\gamma_j E}{\left(E_j^2-E^2\right)^2+\left(\gamma_j E\right)^2}, \tag{4a}$$

$$\tilde{D}_2(E,f_j,E_j,\gamma_j)=E_{\mathrm{p}}^2\frac{2f_j\gamma_j^3E^3}{\left[\left(E_j^2-E^2\right)^2+\left(\gamma_j E\right)^2\right]^2}. \tag{4b}$$

Accordingly, the real part reads:

$$\begin{aligned}\mathrm{Re}[\varepsilon(E,q=0)]_{\mathrm{exp}}&=\varepsilon_1^{(D)}(E,q=0;f_j,E_j,\gamma_j)_{a11\ j}\\&=1+\sum_j^{\mathrm{ioniz}}D_1(E,f_j,E_j,\gamma_j)\\&\quad+\sum_j^{\mathrm{excit}}\tilde{D}_1(E,f_j,E_j,\gamma_j),\end{aligned} \tag{5}$$

where

$$D_1(E,f_j,E_j,\gamma_j)=E_{\mathrm{p}}^2\frac{f_j\left(E_j^2-E^2\right)}{\left(E_j^2-E^2\right)^2+\left(\gamma_j E\right)^2}, \tag{5a}$$

$$\tilde{D}_1(E,f_j,E_j,\gamma_j)=E_{\mathrm{p}}^2\frac{f_j\left(E_j^2-E^2\right)\left[\left(E_j^2-E^2\right)^2+3\left(\gamma_j E\right)^2\right]}{\left[\left(E_j^2-E^2\right)^2+\left(\gamma_j E\right)^2\right]^2}. \tag{5b}$$

Then, the ELF is obtained by

$$\mathrm{Im}\left[\frac{-1}{\varepsilon(E,q=0)}\right]_{\mathrm{exp}}=\frac{\sum_j\varepsilon_2^{(D)}(E,q=0;f_j,E_j,\gamma_j)}{\left(\varepsilon_1^{(D)}(E,q=0;f_j,E_j,\gamma_j)_{a11\ j}\right)^2+\left(\sum_j\varepsilon_2^{(D)}(E,q=0;f_j,E_j,\gamma_j)\right)^2}. \tag{6}$$

In the previous equations, E_{p} is the nominal plasmon energy (21.46, 20.82 and 20.59 eV for liquid water and amorphous and hexagonal ice, respectively). Note that the coefficients f_j, γ_j and E_j in Eqs. (4)–(6) correspond to the (A_j, Γ_j, Ω_j) of the original model proposed by Ritchie and Howie [5]. The notation $D_{1,2}$and $\tilde{D}_{1,2}$ stands for the "normal" and "derivative" forms of the Drude function. In the analytic deconvolution of the experimental optical spectra we used a superposition of four "normal" Drude functions to represent the valence bands with ionization thresholds ($B_{\mathrm{ioniz,min}}$) at 10 eV ($1b_1$), 13 eV ($3a_1$), 17 eV ($1b_2$) and 32 eV ($2a_1$) and five "derivative" Drude functions (which are more sharply peaked) for the discrete excitations which have peak-maxima in the ~8–15 eV range (excitation levels: A^1B_1, B^1A_1, Ryd A + B, Ryd C + D, diffuse bands). The $B_{\mathrm{excit,min}}$ is taken at 7–8 eV (corresponding to the photoabsorption threshold or the band gap). The values of the Drude coefficients f_j, E_j and γ_j for each valence band transition in liquid and solid water may be found in [14] and [16], respectively.

The consistency of the "fitting" procedure is ensured by the fulfillment (to within 1%) of the following sum rules for the normalized number of valence electrons:

$$N_{\mathrm{eff}}^{(v)}=\frac{2}{\pi E_{\mathrm{p}}^2}\int_0^\infty E\,\mathrm{Im}[\varepsilon_{\mathrm{D}}(E,q=0)]\,\mathrm{d}E=1-N_{\mathrm{eff}}^{(\mathrm{K})}, \tag{7a}$$

$$N_{\mathrm{eff}}^{(v)}=\frac{2}{\pi E_{\mathrm{p}}^2}\int_0^\infty E\,\mathrm{Im}\left[\frac{-1}{\varepsilon_{\mathrm{D}}(E,q=0)}\right]\mathrm{d}E=1-N_{\mathrm{eff}}^{(\mathrm{K})}, \tag{7b}$$

where $N_{\mathrm{eff}}^{(\mathrm{K})}=0.178$ [23] is the normalized number of effective K-shell electrons. A further consistency test for the optical-ELF is the calculation of the mean excitation and ionization energy of the stopping power theory, the so-called I-value:

$$\ln(I)=\frac{\int_0^\infty E\ln(E)\mathrm{Im}\left[\frac{-1}{\varepsilon_{\mathrm{D}}(E,0)}\right]\mathrm{d}E}{\int_0^\infty E\,\mathrm{Im}\left[\frac{-1}{\varepsilon_{\mathrm{D}}(E,0)}\right]\mathrm{d}E}. \tag{8}$$

The I-value for the valence bands according to the above optical-data model comes out at 45.7 eV. In contrast to the sum rules (Eqs. (7a) and (7b)) where the K-shell has a minimal contribution, its influence on the I-value is significant. Using a Drude parameterization for the NIST photoelectric data of the oxygen K-shell, the total I-value becomes 82.4 eV in very good agreement with other

theoretical and experimental predictions [14]. Note that whereas the above sum rules are most sensitive to the low energy part of the absorption spectrum, the *I*-value is also sensitive to high energy transfers. Thus, Eqs. (7) and (8) provide a consistency test for the overall reliability of the optical-data model over the entire energy transfer range.

The momentum dependence is introduced by extending *all* three Drude coefficients (*fully*-extended-Drude model) in the sense of: $\varepsilon_D(E,q)=\varepsilon_D(E,q=0;f_j(q),E_j(q),\gamma_j(q))$. Our recent analysis [14] of the experimental data for the Bethe ridge of liquid water has led to the following dispersion relations:

$$f_{\text{excit},j}(q)=f_{\text{excit},j}\lfloor\exp(-a_jq^2)+b_jq^2\exp(-c_jq^2)\rfloor, \tag{9a}$$

$$f_{\text{ioniz},j}(q)=f_{\text{ioniz},j}\frac{1-\sum_j^{\text{excit}}f_{\text{excit},j}(q)}{1-\sum_j^{\text{excit}}f_{\text{excit},j}}, \tag{9b}$$

$$E_{\text{ioniz},j}(q)=E_{\text{ioniz},j}+\frac{q^2}{2m_e}[1-\exp(-cq^d)], \tag{9c}$$

$$\gamma_j(q)=\gamma_j+aq+bq^2, \tag{9d}$$

where the values of the various constants are given in [14].

2.2. The Lindhard dielectric function

The Lindhard dielectric function [9] originally developed for the free-electron gas has been widely used to model the response of the conduction electrons of metals and, in general, of the weakly bound electrons of nearly-free-electron materials [8]. In its standard form it reads:

$$\varepsilon_L(\omega,k)=1+\frac{x^2}{z^2}[f_1(u,z)+\mathrm{i}f_2(u,z)], \tag{10}$$

where $\omega=E/\hbar$, $k=q/\hbar$, $u=\omega/(kv_F)$, $z=k/(2k_F)$, $x^2=e^2/(\pi\hbar v_F)$, and $k_F=m_ev_F/\hbar$ (v_F and k_F are the Fermi velocity and wavenumber, respectively). The functions $f_1(u,z)$ and $f_2(u,z)$, which relate to the real and imaginary parts of the Lindhard dielectric function ε_L, are given by:

$$f_1(u,z)=\frac{1}{2}+\frac{1}{8z}[g(z-u)+g(z+u)], \tag{11a}$$

$$f_2(u,z)=\begin{cases}\frac{\pi}{2}u, & z+u<1\\ \frac{\pi}{8z}[1-(z-u)^2], & |z-u|<1<z+u\\ 0, & |z-u|>1\end{cases}, \tag{11b}$$

where $g(x)=(1-x^2)\ln|(1+x)/(1-x)|$.

Connection with the optical-data model is made by the fact that at the optical limit ($q=0$) the Lindhard-ELF corresponds to a Drude-type function, that is, $\mathrm{Im}[-1/\varepsilon_L(E,q=0;\Gamma_j,\Omega_j)]=D(E,\Gamma_j,\Omega_j)$, which may be used to fit the experimental optical data using Eq. (1). It should be noted that the Lindhard function provides an automatic extension to the momentum space, thus overcoming the need for any empirically derived dispersion expressions.

2.3. The single-pole and δ-oscillator approximations

In the single-pole approximation, the Lindhard dielectric function and its associated ELF read [24]:

$$\varepsilon_L(E,q;E_p)=1+\frac{E_p^2}{E_q^2-E_p^2-E(E+\mathrm{i}\gamma_q)}, \tag{12}$$

$$\mathrm{Im}\left[\frac{-1}{\varepsilon_L(E,q;E_p)}\right]=E_p^2\frac{\gamma_qE}{\left(E_q^2-E^2\right)^2+(\gamma_qE)^2}, \tag{13}$$

where E_p is the plasmon frequency obtained from the electron density, E_q is the dispersion line of a single pole and γ_q is the damping constant. In the limit $\gamma_q\to0$, Eq. (13) becomes a δ-function:

$$\lim_{\gamma_q\to0}\mathrm{Im}\left[\frac{-1}{\varepsilon_L(E,q;E_p)}\right]=\frac{\pi}{2}\frac{E_p^2}{E_q}\delta(E-E_q). \tag{14}$$

As shown by Penn [6] the ELF may be expressed by the following integral:

$$\mathrm{Im}\left[\frac{-1}{\varepsilon(E,q)}\right]=\frac{2}{\pi}\int_0^\infty\mathrm{Im}\left[\frac{-1}{\varepsilon(E_p,0)}\right]\mathrm{Im}\left[\frac{-1}{\varepsilon_L(E,q;E_p)}\right]\frac{\mathrm{d}E_p}{E_p}. \tag{15}$$

Then, using the undamped single-pole approximation of the Lindhard function (Eq. (14)), we may recast Eq. (15) in the form:

$$\mathrm{Im}\left[\frac{-1}{\varepsilon(E,q)}\right]=\int_0^\infty\mathrm{Im}\left[\frac{-1}{\varepsilon(E_p,0)}\right]\frac{\delta(E-E_q)}{E_q}E_p\mathrm{d}E_p, \tag{16}$$

where Penn [6] has suggested the following dispersion relation:

$$E_q^2=E_P^2+\frac{4}{3}E_F(q^2/2m_e)+(q^2/2m_e)^2, \tag{17}$$

where E_F is the Fermi energy. An equivalent expression to Eq. (16) has been formally derived by Fernandez-Varea et al. [8] starting from the more general case of a δ-function expansion of the optical-oscillator-strength. Extension to the q-space may then be provided by an integral over the so-called "δ-oscillator" defined as $\delta(E-F(E';q))$ or, simply, as $\delta(E-E'(q))$. A δ-oscillator representation of the ELF reads:

$$\mathrm{Im}\left[\frac{-1}{\varepsilon(E,q)}\right]=\int_0^\infty\mathrm{Im}\left[\frac{-1}{\varepsilon(E',0)}\right]\frac{\delta(E-E'(q))}{E}E'\mathrm{d}E'. \tag{18}$$

Ashley [7] has proposed a pure quadratic dispersion (similar to Eq. (3b)):

$$E'(q)=E'+\frac{q^2}{2m_e} \tag{19}$$

which resembles the plasmon dispersion of the free-electron gas for small-q, while asymptotically leading to the Bethe-ridge at large-q. It should be noted that the use of a δ-function in Eqs. (16) and (18) greatly simplifies the computational effort for the calculation of subsequent quantities (e.g. inelastic and stopping cross sections). The

similarity of the Penn and Ashley models becomes more obvious when Eqs. (16) and (18) are recast in the form:

$$\mathrm{Im}\left[\frac{-1}{\varepsilon(E,q)}\right]_{\mathrm{Penn,Ashley}} = \frac{E_0}{E}\,\mathrm{Im}\left[\frac{-1}{\varepsilon(E_0)}\right], \tag{20}$$

where E_0 is the positive solution of the dispersion relation $E(q,E_0) = E$ (Eqs. (17) and (19)). Recent applications of the Penn and Ashley models include those of Ziaja et al. [25,26], Tan et al. [27], Tanuma et al. [28], Yue et al. [29], Ding et al. [30], Dapor et al. [31] and Pimblott and LaVerne [32].

2.4. The Mermin dielectric function

The Mermin dielectric function [11] improves upon the Lindhard function in that the finite width of the plasmon peak (i.e. the finite plasmon lifetime) is consistently accounted for and, therefore, a more realistic extension to the momentum space is provided. The Mermin dielectric function ε_M may be written in terms of the Lindhard dielectric function ε_L as follows [33]:

$$\varepsilon_M(E,q) = 1 + \frac{(1+\mathrm{i}\gamma\hbar/E)[\varepsilon_L(E+\mathrm{i}\gamma,q)-1]}{1+(\mathrm{i}\gamma\hbar/E)[\varepsilon_L(E+\mathrm{i}\gamma,q)-1]/[\varepsilon_L(0,q)-1]}, \tag{21}$$

where the γ coefficient is associated with plasmon damping. Similar to the Lindhard model, a connection to the optical data may be made through the equivalence of a Mermin-ELF and a Drude function at the optical limit ($q = 0$). Also, likewise the Lindhard function, the advantage of using the Mermin function lies in that it provides automatically and in a consistent way the extension to the momentum space [11]. Recent applications of the Mermin function to the study of energy loss of swift charged particles in materials with different dielectrical properties may be found in the work of Garcia-Molina, Abril and co-workers [10,34–36].

3. Results and discussion

Since all dielectric models examined practically coincide at the optical limit (leading to a Drude-type optical-ELF), it is of interest here to compare their predictions with respect to the momentum dependence of the ELF which is the essential input in the construction of the Bethe surface. A Drude-type parameterization of the experimental optical data of liquid and solid water (hexagonal and amorphous ice) has been presented in detail elsewhere [14,16] and briefly discussed here following Eq. (6). In the absence of an established band structure model for both liquid water and water ice, a number of approximations had to be adopted in the deconvolution of the optical spectrum to its various electronic channels. The number and type of excitation levels and ionization shells were deduced by the analysis of Kutcher and Green [37] which is based on a molecular-orbital picture of the liquid. However, in view of recent experimental findings [38], the plasmon channel introduced by Kutcher and Green is neglected here. The binding energies for ionization were deduced by lowering the corresponding gas phase values by ~1–2 eV in accordance with recent photoionization experiments [39]. The excitation threshold, which corresponds to the onset of photoabsorption, was loosely associated with the band gap since the extrapolation of the experimental optical data to threshold may entail a relatively larger uncertainty. The band gap values chosen (7–8 eV) fall somewhere in the middle of the theoretical and experimental values found in the literature which vary between about 6 and 12 eV [40–43]. Finally, the adoption of the same band structure characteristics for the liquid and solid phases in terms of number and type of transitions and ionization thresholds, is also a reasonable approximation given that the same molecular orbitals persist in both phases, while

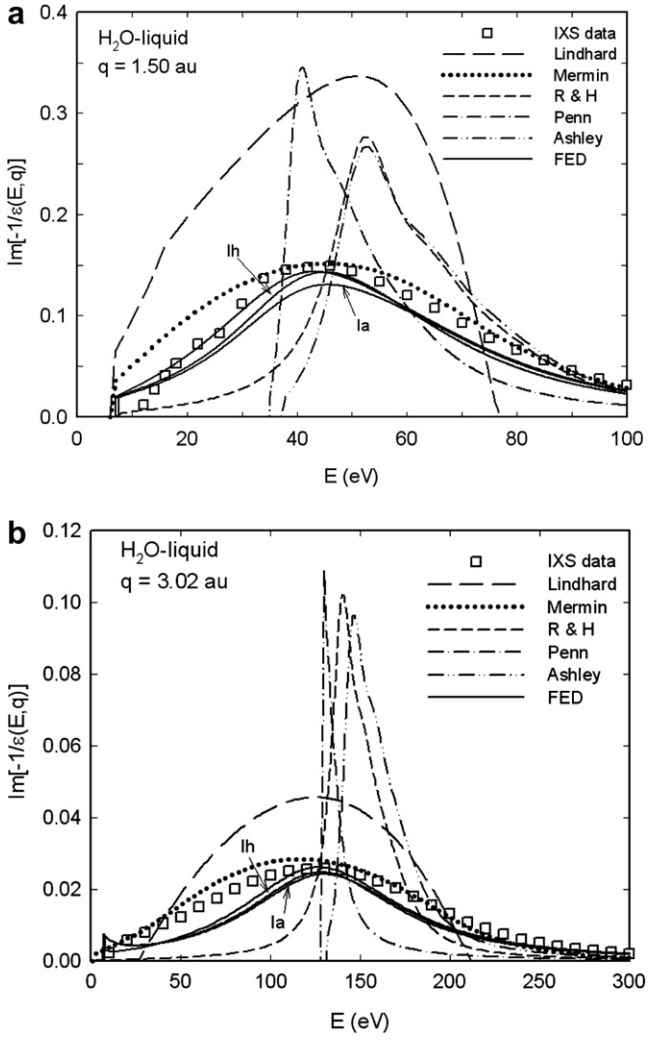

Fig. 1. The energy loss function (ELF) of condensed water for a fixed value of momentum transfer: (a) $q = 1.50$ a.u. or $k = 2.84$ Å^{-1} and (b) $q = 3.02$ a.u. or $k = 5.71$ Å^{-1}. Comparison of experimental IXS data for liquid water [18] and model calculations with several extended-optical-data dielectric models (see text). R&H stands for the Ritchie and Howie model, FED for the fully-extended-Drude model and I_a, I_h for amorphous and hexagonal ice, respectively.

the difference in the ionization potentials is less than 1 eV (those of ice being higher) and, generally, well within their associated uncertainties [39]. The above assumptions are expected to have a minimal effect in the present calculations given that the actual (experimental) optical spectrum for each form of water has been used as input in the extended-optical-data model.

Fig. 1 presents the ELF distribution of condensed water at two finite values of momentum transfer ($q = 1.50$ and 3.02 a.u.; i.e. $k = 2.84$ and 5.71 Å^{-1}) as obtained from the dielectric models examined and the experimental IXS data for liquid water [18] which are reported to have insignificant uncertainties. The FED model calculations [14,16] pertain to both the liquid and solid phase (same dispersion formulae for both phases but different optical data) whereas all other calculations are limited to the liquid phase. As expected, differences between the three forms of condensed water are small and decrease with momentum transfer. With respect to the Ritchie and Howie model [5] we have used its most popular version with the simple quadratic dispersion relation of Eq. (3). Good agreement with the experimental data is observed only in the case of the Mermin [11] and FED models [14,16]. In particular, the more consistent account of plasmon damping in the Mermin function provides a notable improvement over the original Lindhard function [9]. On the other hand, the relatively simple dispersion formulae adopted in the present FED model seem also very effective in reproducing the experimental data while retaining the convenience of working with the Drude function. As noted by Kuhr and Fitting [44] and also confirmed here, the dispersion of the damping-coefficient (Eq. (9d)) provides the expected momentum broadening of the Bethe ridge and results in a notable improvement over earlier extended-Drude models. Moreover, the modified-quadratic dispersion used for the energy-coefficient (Eq. (9c)), shifts the position of the peak to lower energy transfers in better agreement with the experimental data than the pure-quadratic dispersion of the Ritchie and Howie [5] and Ashley [7] models Eqs. ((3) and (19)). A similar effect is also evident in the Penn model [6] which also adopts a weaker momentum dispersion (Eq. (17)). Interestingly, the ELF predicted by the Penn and Ashley models quickly vanishes in the energy transfer range below the peak due to the negative values of E_0 (of Eq. (10)) in this range.

Fig. 2 presents the Bethe surface of liquid water as predicted by the Mermin [11], Ritchie and Howie [5] and FED [14] models. The experimental Bethe surface [18,45] obtained from the IXS measurements is also presented for comparison. As expected from Fig. 1(a),(b) the Mermin and FED models reproduce fairly well the experimental Bethe surface over the whole energy–momentum plane, whereas the Ritchie and Howie model does not exhibit the observed broadening of the Bethe ridge (this is also true for the Lindhard, Penn and Ashley models). It is evident that the momentum broadening effect cannot be repro-

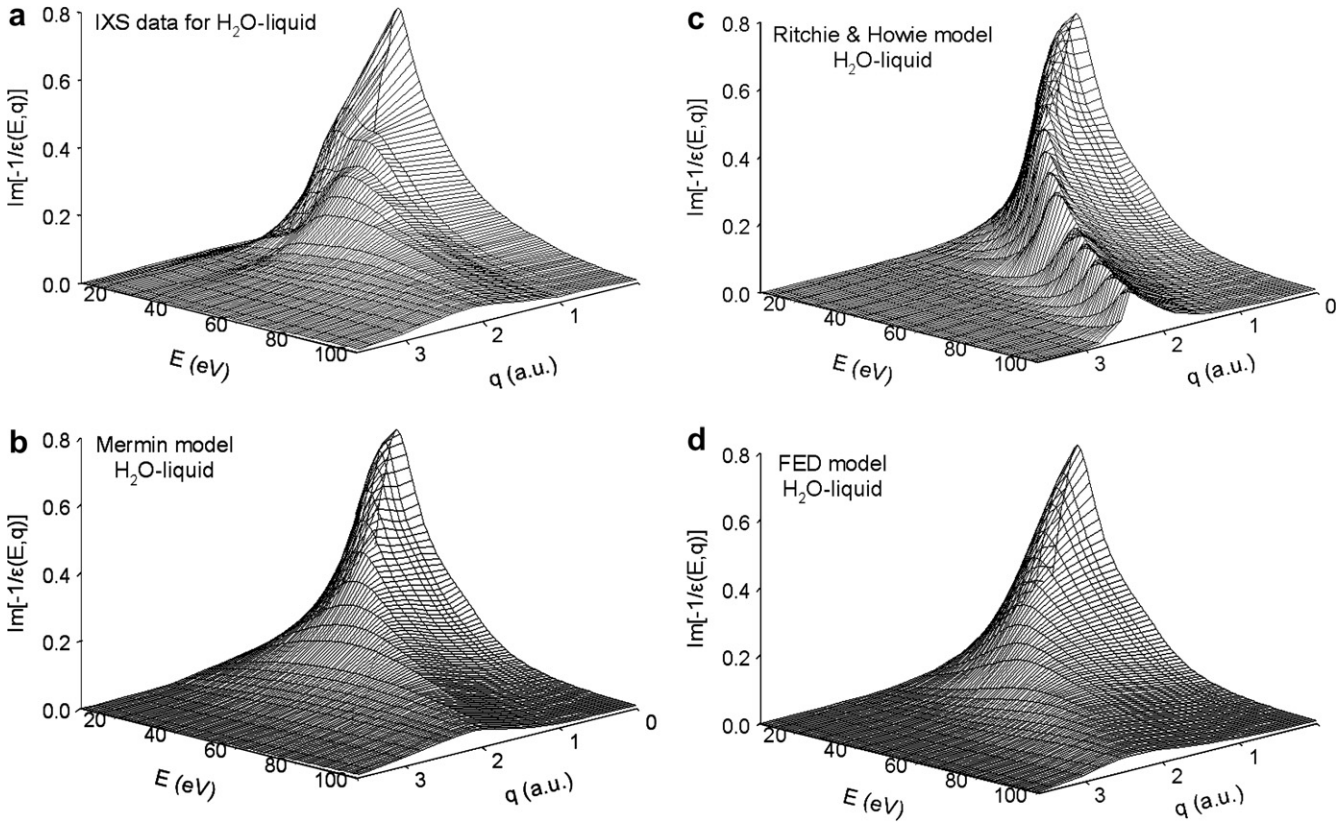

Fig. 2. The Bethe surface of liquid water as determined experimentally by IXS measurements [18,45] and calculated by different extended-optical-data dielectric models (see text).

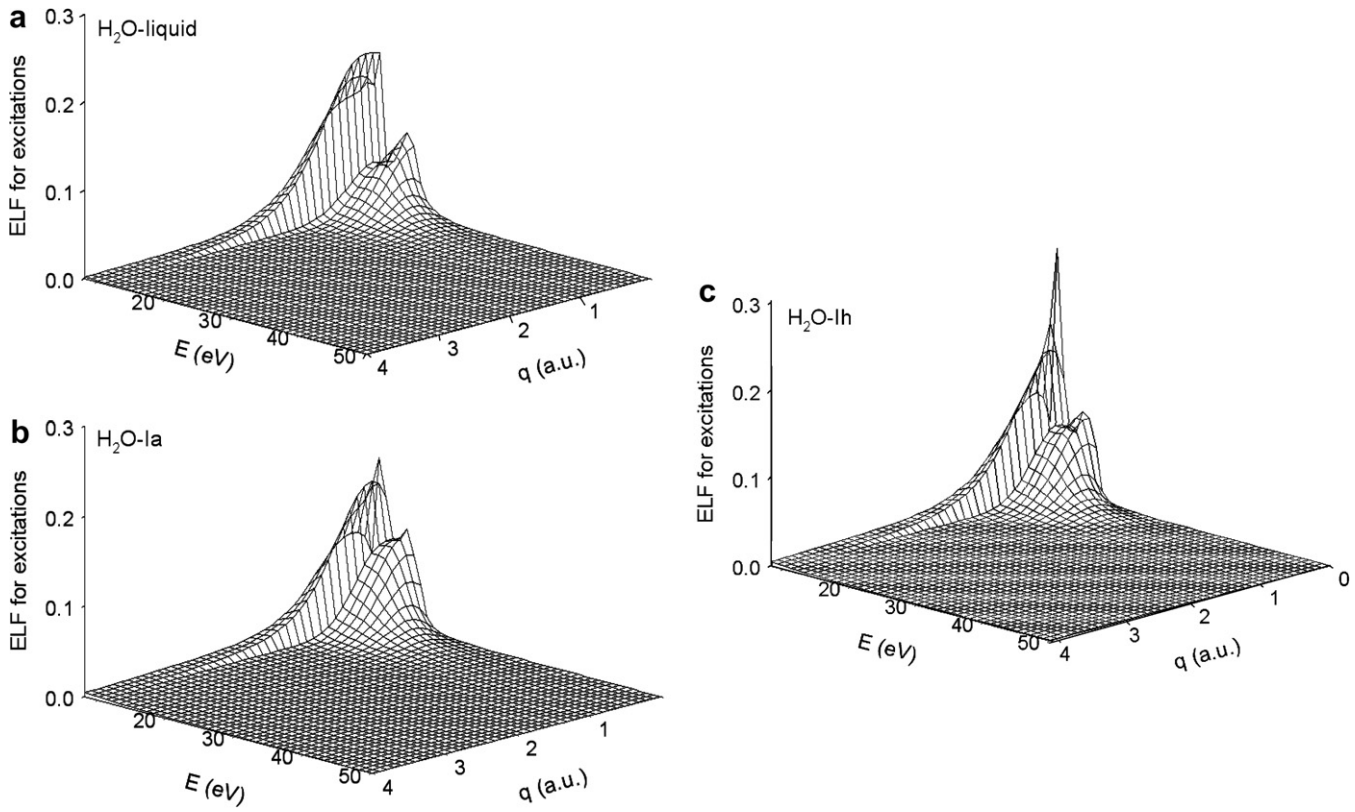

Fig. 3. The excitation part of the Bethe surface of liquid water and water ice (in amorphous and hexagonal form) as determined by the fully-extended-Drude (FED) model [14,16].

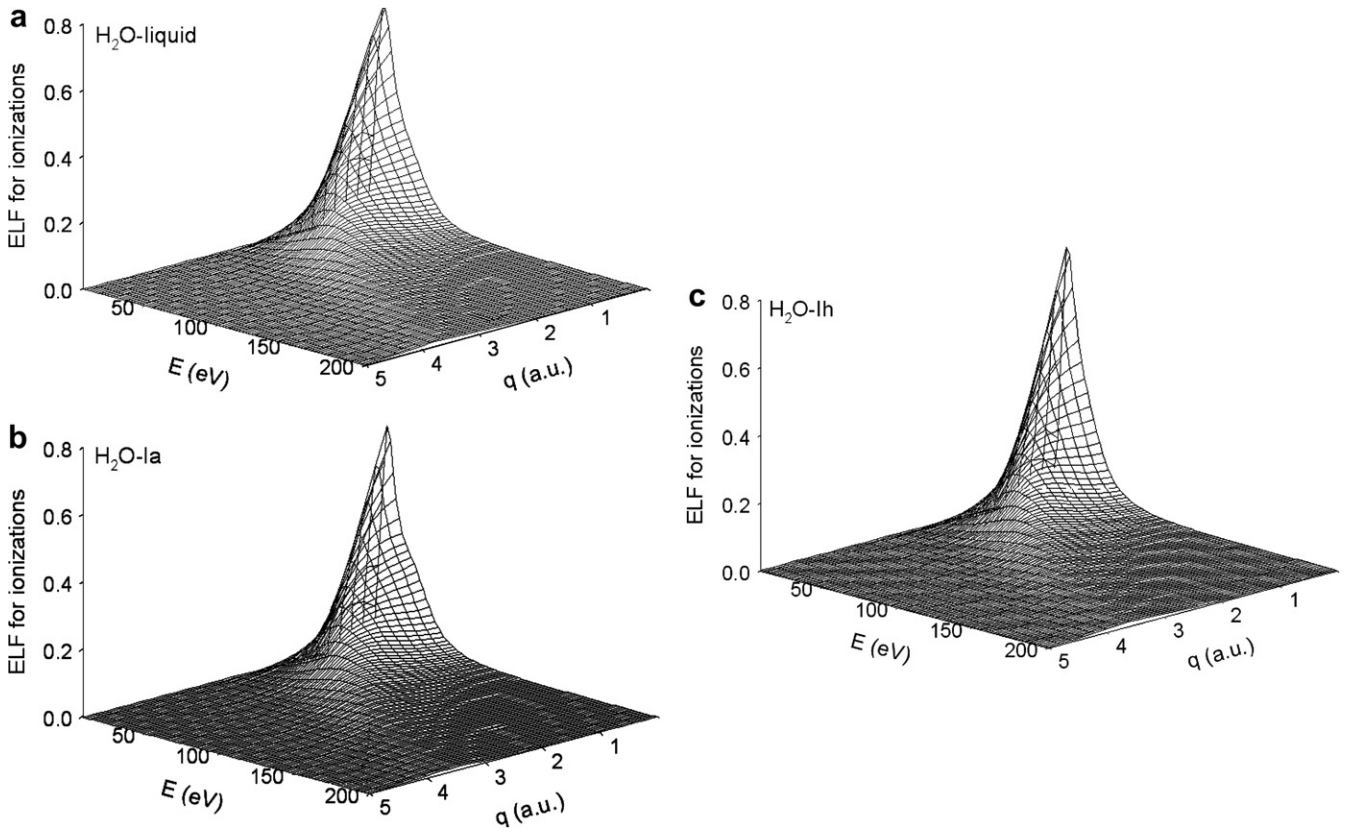

Fig. 4. The ionization part of the Bethe surface of liquid water and water ice (in amorphous and hexagonal form) as determined by the fully-extended-Drude (FED) model [14,16].

duced by any type of energy-dispersion relation alone and some type of a damping-dispersion also needs to be invoked [46,47].

In contrast to most dielectric models which use a transition-invariant form of dispersion [48], the FED model allows us to distinguish in a consistent way between the excitation and ionization parts of the ELF. In Figs. 3 and 4 we present the excitation and ionization parts of the Bethe surface of liquid and solid water as predicted by the FED model (notice the different scale on the vertical axis between excitations and ionizations). The expected damping of the discrete transitions and the concomitant evolution of the Bethe ridge for the continuum is evident in all three forms of condensed water. With increasing momentum transfer the low energy excitation peaks vanish quickly whereas the main absorption peak falls rapidly but does not vanish leading to a broadened Bethe ridge which is gradually displaced at higher values of energy transfer. Differences between the three forms of water are sizeable only for the excitation part since the Bethe ridge (ionization part) is largely indifferent to the details of the electronic structure.

The broadening of the Bethe ridge observed experimentally for both liquid [45] and gaseous [49] water as well as other materials [50] is also consistent with the theoretical expectation that single-particle excitations should gradually prevail over collective excitations with increasing momentum transfer. In fact, using the Lindhard dielectric function one may calculate exactly the critical value of momentum transfer where the sharp plasmon peak is strongly damped by single-particle excitations leading to a momentum-broadened spectrum [33]. Recently, two studies have examined the effect of Bethe ridge characteristics on low-energy electron inelastic cross sections (and associated quantities) and shown to be sizeable [51,52].

Acknowledgement

This work has been partially supported by the Spanish Ministerio de Educación y Ciencia (Projects FIS2006-13309-C02-01 and FIS2006-13309-C02-02).

References

[1] J.M. Fernandez-Varea, F. Salvat, M. Dingfelder, D. Liljequist, Nucl. Instr. and Meth. B 229 (2005) 187.
[2] S. Segui, M. Dingfelder, J.M. Fernandez-Varea, F. Salvat, J. Phys. B: At. Mol. Opt. Phys. 35 (2002) 33.
[3] M. Inokuti, Rev. Mod. Phys. 43 (1971) 297.
[4] J.M. Fernandez-Varea, Radiat. Phys. Chem. 53 (1998) 235.
[5] R.H. Ritchie, A. Howie, Philos. Magazine 36 (1977) 463.
[6] D.R. Penn, Phys. Rev. B 35 (1987) 482.
[7] J.C. Ashley, J. Electron Spectrosc. Relat. Phenom. 46 (1988) 199.
[8] J.M. Fernandez-Varea, R. Mayol, F. Salvat, D. Liljequist, J. Phys.: Cond. Mat. 4 (1992) 2879.
[9] J. Lindhard, Kgl. Dan. Vidensk. Mat. Fys. Medd. 28 (1954) 1.
[10] I. Abril, R. Garcia-Molina, C.D. Denton, J. Pérez-Pérez, N.R. Arista, Phys. Rev. A 58 (1998) 357.
[11] N.D. Mermin, Phys. Rev. B 1 (1970) 2362.
[12] D. Emfietzoglou, Radiat. Phys. Chem. 66 (2003) 373.
[13] D. Emfietzoglou, H. Nikjoo, Radiat. Res. 163 (2005) 98.
[14] D. Emfietzoglou, F. Cucinotta, H. Nikjoo, Radiat. Res. 164 (2005) 202.
[15] D. Emfietzoglou, H. Nikjoo, A. Pathak, Radiat. Prot. Dosim. 122 (2006) 61.
[16] D. Emfietzoglou, H. Nikjoo, I.D. Petsalakis, A. Pathak, Nucl. Instr. and Meth. B 256 (2007) 141.
[17] H. Hayashi, N. Watanabe, Y. Udagawa, C.-C. Kao, Proc. Natl. Acad. Sci. USA 97 (2000) 6264.
[18] N. Watanabe, H. Hayashi, Y. Udagawa, Bull. Chem. Soc. Jpn. 70 (1997) 719.
[19] J. Leger, M. Yousfi, O. Eichwald, J.F. Loiseau, B. Held, J. Phys. D: Appl. Phys. 38 (2005) 1005.
[20] A. Akkerman, J. Barak, D. Emfietzoglou, Nucl. Instr. and Meth. B 227 (2005) 319.
[21] C.J. Tung, T.C. Chao, H.W. Hsieh, W.T. Chen, Nucl. Instr. and Meth. B 262 (2007) 231.
[22] M. Dingfelder, D. Hantke, M. Inokuti, H.G. Paretzke, Radiat. Phys. Chem. 53 (1998) 1.
[23] M. Inokuti, J.L. Dehmer, T. Baer, H.D. Hanson, Phys. Rev. A 23 (1981) 95.
[24] Z.-J. Ding, R. Shimizu, Surf. Sci. 222 (1989) 313.
[25] B. Ziaja, D. van der Spoel, A. Szoke, J. Hajdu, Phys. Rev. B 64 (2001) 214104-1.
[26] B. Ziaja, A. Szoke, D. van der Spoel, J. Hajdu, Phys. Rev. B 66 (2002) 024116-1.
[27] Z. Tan, Y. Xia, M. Zhao, X. Liu, F. Li, B. Huang, Y. Li, Nucl. Instr. and Meth. B 222 (2004) 27.
[28] S. Tanuma, C.J. Powell, D.R. Penn, Surf. Interf. Anal. 37 (2005) 978.
[29] Y.T. Yue, H.M. Li, Z.J. Ding, J. Phys. D: Appl. Phys. 38 (2005) 1966.
[30] Z.J. Ding, K. Salma, H.M. Li, Z.M. Zhang, K. Tokesi, D. Varga, J. Toth, K. Goto, R. Shimizu, Surf. Interf. Anal. 38 (2006) 657.
[31] M. Dapor, Surf. Interf. Anal. 38 (2006) 1198.
[32] S.M. Pimblott, J.A. LaVerne, Radiat. Phys. Chem. 76 (2007) 1244.
[33] D.J. Planes, R. Garcia-Molina, I. Abril, N.R. Arista, J. Electron Spectrosc. Relat. Phenom. 82 (1996) 23.
[34] S. Heredia-Avalos, R. Garcia-Molina, J.M. Fernandez-Varea, I. Abril, Phys. Rev. A 72 (2005) 052902.
[35] S. Heredia-Avalos, J.C. Moreno-Marín, I. Abril, R. Garcia-Molina, Nucl. Instr. and Meth. B 230 (2005) 118.
[36] J.C. Moreno-Marín, I. Abril, R. Garcia-Molina, Nucl. Instr. and Meth. B 193 (2002) 30.
[37] G.J. Kutcher, A.E.S. Green, Radiat. Res. 67 (1976) 408.
[38] C.D. Wilson, C.A. Dukes, R.A. Baragiola, Phys. Rev. B 63 (2001) 121101.
[39] B. Winter, R. Weber, W. Widdra, M. Dittmar, M. Faubel, I.V. Hertel, J. Phys. Chem. A 108 (2004) 2625.
[40] I.G. Kaplan, A.M. Miterev, Adv. Chem. Phys. 68 (1987) 255.
[41] V.F. Petrenko, I.A. Ryzhkin, Phys. Rev. Lett. 71 (1993) 2626.
[42] A. Mozumder, Phys. Chem. Chem. Phys. 4 (2002) 1451.
[43] P.H. Hahn, W.G. Schmidt, K. Seino, M. Preuss, F. Bechstedt, J. Bernholc, Phys. Rev. Lett. 94 (2005) 037404-1.
[44] J.-Ch. Kuhr, H.-J. Fitting, Phys. Stat. Sol. a 172 (1999) 433.
[45] N. Watanabe, H. Hayashi, Y. Udagawa, J. Phys. Chem. Solids 61 (2000) 407.
[46] Z.-J. Ding, R. Shimizu, Scanning 18 (1996) 92.
[47] M. Dingfelder, M. Inokuti, Radiat. Environ. Biophys. 38 (1999) 93.
[48] J.-C. Kuhr, H.-J. Fitting, J. Electron Spectrosc. Relat. Phenom. 105 (1999) 257.
[49] M. Takahashi, N. Watanabe, Y. Wada, S. Tsuchizawa, T. Hirosue, H. Hayashi, Y. Udagawa, J. Electron Spectrosc. Relat. Phenom. 112 (2000) 107.
[50] G. Tirao, G. Stutz, V.M. Silkin, E.V. Chulkov, C. Cusatis, J. Phys.: Condens. Mat. 19 (2007) 046207.
[51] D. Emfietzoglou, H. Nikjoo, Radiat. Res. 167 (2007) 110.
[52] W. de la Cruz, F. Yubero, Surf. Interf. Anal. 39 (2007) 460.